UDC 669.162.275.2 DOI: 10.70769/2181-7383.MBU.1(104).2026.11

CHARACTERIZATION OF CALCIUM-RICH STEEL SLAG WITH FLUORINE-BEARING MICRODOMAINS

Mardonov B.T.,
Rector of the Navoi State University of Minng and Technologies, DSc, Professor

Sayfidinova M.Kh.,
Navoi State University of Minng and Technologies, PhD student

Abstract. *In this study, steel slag particles were examined by scanning electron microscopy (SEM) coupled with energy-dispersive X-ray spectroscopy (EDS) to clarify how micro-scale morphology relates to local chemical composition. High-magnification secondary-electron images showed that the slag consists predominantly of angular, brittle fragments with sharp edges and irregular particle outlines, which is typical of rapid fracture of heterogeneous, hard phases. Many surfaces exhibited lamellar, stepped, or cleavage-like features, indicating preferential crack propagation along phase boundaries or crystallographic planes. In addition, numerous fine particles were observed adhering to larger fragments and accumulating in surface recesses, suggesting either mechanical attrition during handling/grinding or the presence of weakly bonded secondary phases. The coexistence of smooth, plate-like regions and more granular, porous zones supports the interpretation of a multi-phase material with localized differences in toughness and fracture mechanisms.*

Elemental characterization was performed using an EDS map-sum spectrum collected from a representative area of the particle surface. The spectrum was dominated by calcium, evidenced by a strong Ca Kα peak, accompanied by oxygen as the second major component, consistent with a matrix rich in Ca-bearing oxides and/or silicates. A noticeable fluorine contribution was also detected, implying the presence of fluoride-containing phases or residual flux-related compounds introduced during steelmaking and slag conditioning. Silicon and magnesium appeared as minor constituents, which may reflect limited amounts of silicate phases and Mg-bearing oxides/spinels dispersed within the Ca-rich matrix. Manganese was detected only at trace level, suggesting either dilute substitution in oxide phases or small inclusions below the spatial resolution of the map-sum area.

Keywords: *scanning electron microscope, slags, steel, manganize, silicon.*

FTOR TUTUVCHI MIKRODOMENLARGA EGA BO‘LGAN KALSIYGA BOY PO‘LAT ISHLAB CHIQARISH SHLAKINI XUSUSUYATINI O‘RGANISH

Mardonov B.T., Sayfidinova M.X.

Navoiy davlat konchilik va texnologiyalar universiteti, O‘zbekiston Respublikasi

Annotatsiiya. *Ushbu tadqiqotda po‘lat shlagi zarralari skanerlovchi elektron mikroskopiya (SEM) va energiya-dispersiv rentgen spektroskopiyasi (EDS) bilan birgalikda qo‘llanib, mikroko‘lamdagi morfologiya bilan mahalliy kimyoviy tarkib o‘rtasidagi bog‘liqlik aniqlashtirildi. Katta kattalashtirishdagi ikkilamchi elektron tasvirlari shlak asosan burchakli, mo‘rt bo‘lakchalardan iborat ekanini ko‘rsatdi; ularning qirralari o‘tkir, zarra konturlari esa notekis bo‘lib, bu geterogen va qattiq fazalarning tez sinishi uchun xos holatdir. Ko‘plab yuzalarda lamellar (qatlamli), pog‘onali yoki yoriqlanishga o‘xshash (cleavage-like) belgilar kuzatildi, bu esa yoriqlar faza chegaralari yoki kristallografik tekisliklar bo‘ylab ustuvor tarqalishini anglatadi. Bundan tashqari, yirik bo‘lakchalarga yopishib qolgan va yuzadagi chuqurcha hamda notekis joylarda to‘plangan ko‘plab mayda zarrachalar aniqlandi; bu ularni tashish/tegirmonlash jarayonida mexanik yemirilish (attritsiya) sodir bo‘lganini yoki mustahkam bog‘lanmagan ikkilamchi fazalar mavjudligini ko‘rsatishi mumkin. Silliq, plastinkasimon (yassi) sohalar bilan birga donador va g‘ovak zonalarning ham uchrashi materialning ko‘p fazali ekanini hamda mahalliy mustahkamlik va sinish mexanizmlarida farqlar mavjudligini tasdiqlaydi.*

Element tarkibini aniqlash zarra yuzasining vakillik qiluvchi qismidan olingan EDS “map-sum” spektri asosida bajarildi. Spektrda kalsiy ustun bo‘lib, bu kuchli Ca Kα cho‘qqisi bilan tasdiqlandi; kislorod esa ikkinchi asosiy komponent sifatida qayd etildi, bu Ca tarkibli oksidlar va/yoki silikatlarga boy matritsa mavjudligiga mos keladi. Shuningdek, sezilarli miqdorda ftor signali ham aniqlandi; bu po‘lat ishlab chiqarish va shlakni konditsiyalash jarayonida kirib qolgan ftorli fazalar yoki flux (shlak hosil qiluvchi qo‘shimchalar) bilan bog‘liq qoldiq birikmalar borligini anglatishi mumkin. Kremniy va magniy kichik komponentlar sifatida kuzatildi, bu Ca ga boy matritsa ichida cheklangan miqdordagi silikat fazalari hamda Mg tarkibli oksidlar/shpinellar tarqalganini ko‘rsatishi mumkin. Marganes esa faqat iz (trace) darajada qayd etildi; bu uning oksid fazalarda juda kam miqdorda izomorf almashinuvi sifatida mavjudligini yoki “map-sum” hududining fazoviy aniqligi doirasidan kichik bo‘lgan mayda qo‘shimcha inkluziyalar borligini taxmin qiladi.

Kalit so‘zlar: *skanerlash elektron mikroskopi, shlaklar, po‘lat, marganets, kremniy.*

ХАРАКТЕРИЗАЦИЯ КАЛЬЦИЙСОДЕРЖАЩЕГО СТАЛЕПЛАВИЛЬНОГО ШЛАКА С ФТОРСОДЕРЖАЩИМИ МИКРОДОМЕНАМИ

Мардонов Б.Т., Сайфидинова М.Х.

Навоийский государственный горно-технологический университет, Республика Узбекистан

Аннотация. В данном исследовании частицы стального шлака изучались с помощью растровой электронной микроскопии (РЭМ) в сочетании с энергодисперсионной рентгеновской спектроскопией (EDS) для выяснения взаимосвязи микроструктуры с локальным химическим составом. Изображения, полученные в режиме вторичных электронов при высоком увеличении, показали, что шлак состоит преимущественно из угловатых, хрупких фрагментов с острыми краями и неправильной формой частиц, что характерно для быстрого разрушения гетерогенных твердых фаз. Многие поверхности демонстрировали ламеллярные, ступенчатые или подобные трещине структуры, что указывает на преимущественное распространение трещин вдоль границ фаз или кристаллографических плоскостей. Кроме того, на поверхности крупных фрагментов наблюдались многочисленные мелкие частицы, прилипшие и накопившиеся в углублениях, что может свидетельствовать либо о механическом истирании при обработке/измельчении, либо о наличии слабо связанных вторичных фаз. Сосуществование гладких, пластинчатых областей и более зернистых, пористых зон поддерживает интерпретацию материала как многокомпонентного с локальными различиями в прочности и механизмах разрушения.

Элементный состав был охарактеризован с помощью суммарного спектра EDS, полученного с представительной области поверхности частицы. Спектр был доминирован кальцием, о чём свидетельствует яркий пик Ca Kα, сопровождаемый кислородом в качестве второго по значимости компонента, что соответствует матрице, богатой оксидами кальция и/или силикатами. Также была отмечена заметная концентрация фтора, что предполагает наличие фторсодержащих фаз или остаточных соединений флюса, введённых в процессе сталеплавильного производства и кондиционирования шлака. Кремний и магний присутствовали в меньших количествах, что может отражать ограниченное содержание силикатных фаз и Mg-оксидов/спинелей, распределённых в Ca-богатой матрице. Марганец был обнаружен лишь в следовых количествах, что может указывать либо на его разреженное замещение в оксидных фазах, либо на наличие мелких включений ниже пространственного разрешения области суммарного спектра.

Ключевые слова: растровый электронный микроскоп, шлаки, сталь, марганцевый, кремний.

Steel slag is a byproduct generated during the steelmaking process, especially from electric arc furnaces (EAF) and basic oxygen furnaces (BOF). As a major byproduct of modern steel production, steel slag accounts for about 150 kg per tonne of steel, making its management and reuse vital for addressing environmental concerns associated with industrial waste. The unique chemical composition and physical properties of steel slag offer various potential uses, notably in construction, agriculture, and environmental cleanup, emphasizing its importance as a valuable resource in a circular economy. The composition of steel slag varies widely and depends on factors such as the type of steel produced, the raw materials used, and the operational conditions of the furnace. Common chemical components include calcium oxide, silicon dioxide, and various metal oxides, which contribute to its structural strength and usability. Steel slag has gained attention for its role in reducing dependency on natural aggregates, improving soil quality in agricultural practices, and serving as an effective material for carbon capture and remediation projects. However, concerns about the leaching of heavy metals and the environmental impacts associated with their use require careful evaluation and management. As industries increasingly prioritize sustainability, recycling and beneficial reuse of steel slag align with global environmental goals. The adoption of innovative technologies and practices in steel production is expected to further enhance steel slag's role in advancing a more sustainable future while addressing urgent challenges in waste management and environmental degradation. Despite its potential benefits, the use of steel slag is not without controversy. Issues related to the environmental impacts of leaching harmful elements and the need for regulatory oversight present challenges to the widespread acceptance and application of this technology. Ongoing research and advancements in processing technologies are essential to mitigate these risks and unlock the full potential of steel slag as a valuable resource across various industries. Chemical Composition discussion

Materials and methods

The main chemical components of steel slag include oxides such as calcium oxide (CaO), silicon dioxide (SiO_2), iron oxides (FeO, Fe_2O_3), magnesium oxide (MgO), and aluminum oxide (Al_2O_3) [1, 2]. Other components, including manganese oxide (MnO) and phosphorus pentoxide (P_2O_5), are also present, but in smaller amounts [3] [4]. The composition of steel slag is usually expressed as simple oxides obtained from elemental analysis, with most steel slags falling within established chemical ranges [5]. Variability in slag composition mainly results from differences in metallurgical processes and raw materials. For example, EAF slag often contains significant amounts of lime and other oxides produced during melting and refining, which are necessary to remove impurities and achieve the desired steel quality [6, 7].

To organize the laboratory investigations, steel slag was collected directly from the waste management area of the Navoi Machine Building Plant (NMBP), where the material is temporarily stored after production operations. To minimize compositional bias and ensure that the analyzed particles were representative of the bulk waste stream, the sampling procedure targeted several points within the storage zone and included fragments with visually different colors and textures. The collected slag was transported to the laboratory in sealed containers to reduce additional contamination from dust and to preserve the as-received surface condition as much as possible.

In the laboratory, the slag was mechanically reduced in size using a specialized crushing machine. The crushing step was selected to generate fresh fracture surfaces and to obtain particle fractions suitable for subsequent handling and imaging. After crushing, the material was sieved into two granulometric ranges—approximately 2.36–4.75 mm and 4.75–9.5 mm—which were then used as the primary specimens for examining the surface texture of the raw slag. These size intervals were chosen because they (i) provide sufficient surface area and morphological features for SEM observation, (ii) are easy to mount without additional grinding or polishing, and (iii) allow evaluation of heterogeneity between coarse and medium fractions that may differ in phase distribution or fracture behavior.

For SEM analysis, individual particles were selected from each size fraction and mounted on aluminum SEM stubs using electrically conductive, non-porous carbon adhesive tapes. The use of conductive

carbon tape ensured stable fixation of irregular fragments and provided a continuous pathway for electron discharge, which is essential for minimizing charging artifacts during electron-beam exposure—particularly for oxide-rich or partially insulating slag phases. In cases where a specific particle orientation or a defined region of interest was required (e.g., freshly fractured face, lamellar area, or region with adhered fines), the fragments were gently pressed into the tape to improve mechanical stability without altering the surface relief. No polishing or chemical cleaning was applied so that the SEM micrographs would reflect the intrinsic surface morphology of the crushed slag. Prior to imaging, the mounted samples were inspected visually and lightly blown with clean air to remove loose dust particles that could obscure microstructural features; however, strongly adhered fines were intentionally retained, as they can provide information about secondary phase detachment and attrition behavior.

After sample preparation, the slag particles were examined using scanning electron microscopy (SEM) combined with energy-dispersive X-ray spectroscopy (EDS) in order to characterize surface morphology and evaluate local chemical heterogeneity at the micrometer and submicrometer scales. SEM observations were performed on a Thermo Scientific Apreo 2 microscope using secondary-electron (SE) imaging with an Everhart–Thornley detector (ETD). This detector configuration was selected because it provides strong topographic sensitivity, allowing fracture steps, lamellar patterns, microcracks, and attached fine particles to be clearly distinguished. The representative micrograph shown in Fig. 1 was acquired at 10,000× magnification (scale bar: 5 μm) under the following operating conditions: accelerating voltage (HV) = 15.00 kV, beam current = 1.6 nA, and working distance (WD) = 8.07 mm (standard operating conditions). These parameters offer a practical balance between image resolution and signal intensity, delivering high topographic contrast while maintaining sufficient electron-beam energy for reliable EDS microanalysis of major and minor inorganic constituents. The chosen accelerating voltage also supports excitation of characteristic X-ray lines for typical slag-forming elements (e.g., Ca, Si, Mg, Mn, and others), enabling the correlation of morphological features with localized compositional variations.

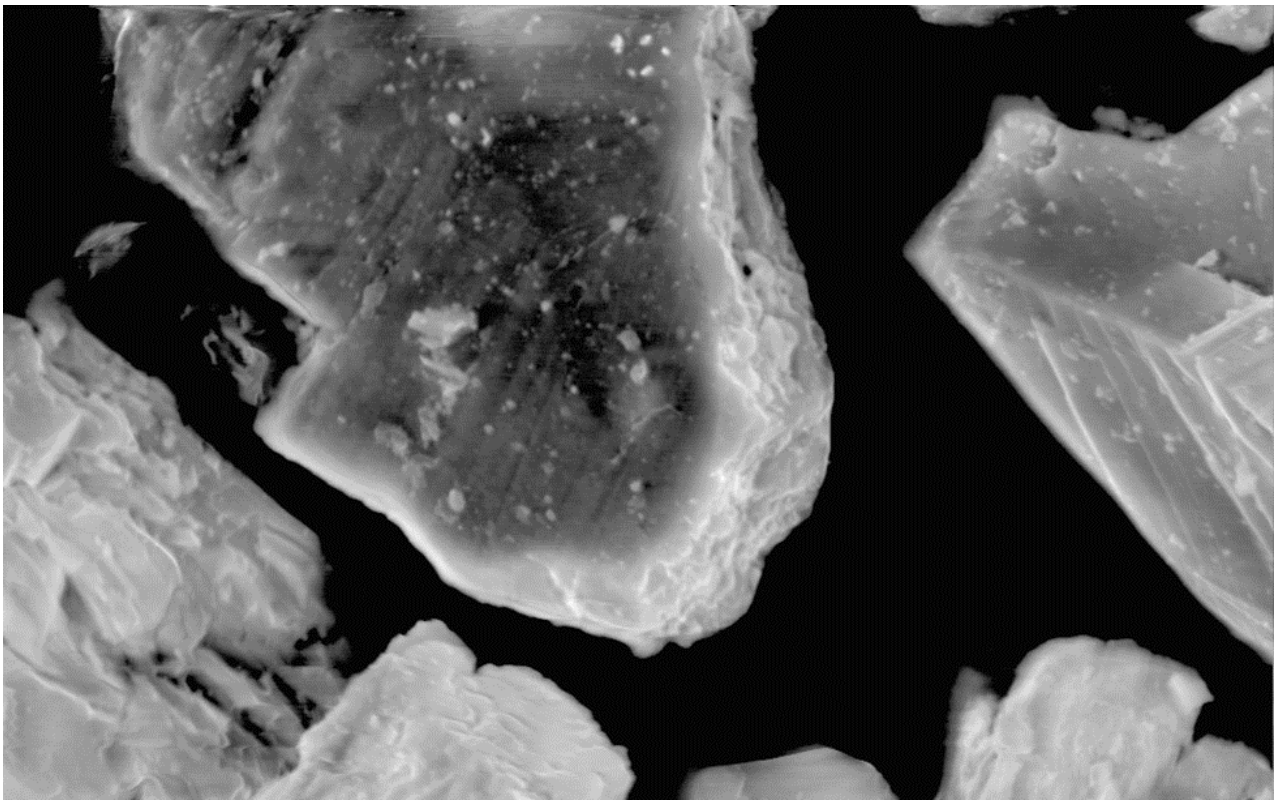

Figure 1. Electron picture of SEM–EDS characterization of steel slag (Thermo Scientific Apreo 2)

Results

The EDS map-sum spectrum obtained from the selected steel slag region indicates a composition strongly dominated by calcium, accompanied by oxygen and a clearly detectable fluorine contribution, together with minor signals attributable to silicate- and oxide-forming elements. The most intense feature of the spectrum is the Ca Kα peak centered at approximately 3.69 keV, accompanied by the Ca Kβ line (observed as a shoulder near 4.01 keV). The prominence of these calcium lines confirms that the analyzed area is composed primarily of Ca-bearing phases, which are commonly reported in steelmaking slags as calcium-rich oxides and calcium silicates (e.g., lime-derived phases and Ca–Si–O compounds). In practical terms, such a Ca-dominated signature typically reflects either unreacted or partially reacted lime and/or Ca-rich reaction products formed during high-temperature slag generation and subsequent cooling.

At lower energies, the spectrum shows two characteristic peaks for oxygen and fluorine: O Kα at approximately 0.52 keV and F Kα at around 0.68 keV. The oxygen peak aligns with the dominance of oxide-based minerals and confirms that the main phases in the sampled area are oxidized rather than metallic. The fluorine peak, though smaller than those of calcium and oxygen, remains clearly distinguishable, indicating the presence of fluorine-containing compounds above the

detection limit of the EDS measurement. This is significant because fluorine in steel slags is typically linked to fluxing agents or process additives (such as fluoride compounds used to alter slag viscosity and melting properties). The concurrent presence of Ca, O, and F suggests that part of the analyzed micro-area may contain Ca–F–O phases or fluoride-bearing calcium compounds formed during slag processing and cooling. Additionally, fluorine might appear as isolated fluoride inclusions or as part of complex Ca-rich matrices, depending on local chemistry and thermal history.

Apart from the dominant Ca–O–F signals, weaker peaks—previously noted in the broader dataset—corresponding to elements like Si and Mg support the existence of minor silicate and magnesium oxide phases dispersed within the Ca-rich background. Although these peaks are small, they indicate chemical heterogeneity at the micro-scale, suggesting that the slag is a multiphase material rather than a single phase, with Ca-rich areas coexisting alongside silicate- and oxide-based components. This phase mixing influences fracture behavior, grinding, and potential reactivity during reuse, such as in glass-ceramics or secondary raw materials. Overall, the spectrum confirms that the area mainly consists of a Ca-rich oxide matrix with notable fluorine, aligning with typical steelmaking slag chemistry and the possible retention of fluoride from flux inputs during processing.

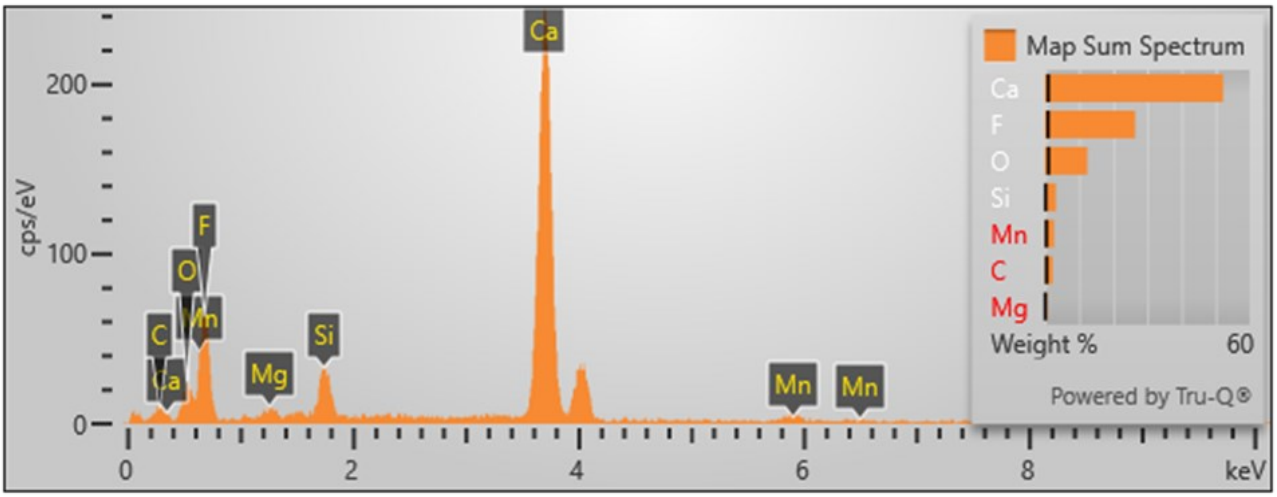

Figure 2. EDS map-sum spectrum of steel slag (SEM–EDS)

The spectrum shows two small peaks corresponding to Mg Kα radiation at 1.25 keV and Si Kα radiation at 1.74 keV, indicating that only a small amount of Mg-Si containing phases (such as silicates or mixed Ca-Mg-Si oxides) exist in the measured region. The presence of Mn is detected at minimal concentrations because the Kα (~5.90 keV) and Kβ (~6.49 keV) peaks of Mn appear in the spectrum, which is consistent with the behavior of steelmaking slags that form oxide phases containing Mn. The C peak shows a small signal at 0.28 keV, resulting from surface carbon contamination and the use of conductive carbon coating or tape. Careful analysis of this signal is necessary to interpret the intrinsic slag chemistry, as it originates from surface contamination. The accompanying semi-quantitative bar plot (map-sum, weight %) aligns with these findings: Ca is the predominant element, followed by F and O, while Si, Mg, Mn, and C are minor to trace components in the mapped region. The slag area mainly consists of Ca-rich oxide and fluoride phases, along with small amounts of silicate materials and Mn-bearing oxides as indicated by the spectrum.

Discussion

The performance of steel slag in reuse and valorization routes is largely governed by its metallurgical origin and cooling history, which collectively determine phase assemblage, microstructure, and local chemical variability. Unlike conventional single-phase mineral raw materials, steel slag forms through a high-temperature, chemically dynamic process where lime, silica, alumina, magnesia, and minor alloying/impurity elements react under strongly oxidizing conditions. During tapping and subsequent cooling, the melt solidifies rapidly and often non-uniformly, generating a multiphase material in which Ca-rich oxides, calcium silicates, and Mg- or Mn-containing oxides may coexist at the micrometer scale. As a result, steel slag typically exhibits strong spatial heterogeneity in both composition and mechanical response, which in turn controls its grinding behavior, leaching tendency, and suitability for applications such as construction aggregates, cementitious binders, glass-ceramics, and functional fillers.

The SEM micrograph of the investigated steel slag (10,000×; 5 μm scale bar) shows a highly irregular brittle fracture pattern characterized by angular fragments with sharp edges, stepped fracture facets, and localized cleavage-like or lamellar surfaces. These features are typical of fracture in heterogeneous oxide–silicate systems, where cracks tend to follow phase boundaries or pass through brittle crystalline grains with clear cleavage tendencies. The presence of lamellar and plate-like regions indicates that certain slag phases fracture in a layered way, while the more granular and jagged areas suggest either a finer multiphase mixture or regions with pores, microcracks, and weaker interfaces. This variety of morphologies is common in steelmaking slags, because rapid solidification and air cooling lead to a non-equilibrium microstructure: some phases crystallize early and create coarse, brittle zones, while later solidification produces finer intergrowths or glassy/partially amorphous matrices. As a result, even within a single particle, the fracture behavior can vary greatly depending on the phase distribution and the presence of microdefects caused by cooling.

A consistent observation is that fine particles attach to larger fragments and accumulate in surface recesses. These fines can originate from secondary breakage during crushing and handling, but their ten-

dency to adhere to certain surfaces also suggests microstructural causes. For instance, weakly bonded secondary phases or microcracked areas detach more easily, generating fine debris that either sticks electrostatically or becomes mechanically trapped in asperities. This feature is significant because the fine fraction often increases the specific surface area, enhancing reactivity, dissolution kinetics, and sintering behavior. However, a high amount of adhered fines can complicate separation and classification, affect flowability in powder processing, and impact product consistency if the fines differ in composition from coarser phases. The microstructural heterogeneity observed supports previous findings that steel slag is inherently multiphase, with phase composition and microtexture depending on production practices like furnace type, flux additions, and slag conditioning. In practical reuse applications, this heterogeneity has two main implications. First, chemical variability affects reactivity: Ca-rich oxide and silicate phases are typically more prone to hydration, carbonation, or dissolution than more stable spinel-like or Mg-rich oxides, leading to uneven reaction fronts in cementitious or environmental uses. Second, microstructural differences influence mechanical behavior and crushing: brittle, coarse crystalline phases fracture easily and create angular particles, while finer intergrowths and glassy regions fracture differently, resulting in a wider size range. Both aspects influence downstream processing choices such as milling energy, classification methods, and the necessity for pre-treatment (washing, aging, or thermal conditioning).

Overall, the SEM evidence supports the interpretation that the investigated slag is a structurally complex material formed by rapid solidification of multiple oxide and silicate phases. This complexity is not merely a descriptive feature; it influences slag performance in reuse applications. Therefore, any valorization pathway should explicitly consider (i) phase-dependent fracture behavior and surface texture, (ii) the distribution and composition of fine attached particles, and (iii) local chemical heterogeneity that can cause uneven reactivity. In future work, correlating these SEM observations with quantitative phase analysis (e.g., XRD with Rietveld refinement) and localized EDS mapping across multiple regions would further strengthen the connection between microstructure, composition, and application-specific performance.

Conclusion

The SEM images revealed that steel slag particles exhibit a wide variety of microstructural features because they contain multiple angular, brittle fragments with local lamellar and cleavage-like surfaces, along with small particulate inclusions. The material's multiphase composition is demonstrated by these microscopic features. The SEM–EDS map spectrum from the analyzed region showed strong calcium signals combined with oxygen and fluorine, and smaller amounts of silicon and magnesium, as well as trace amounts of manganese. The examined slag area contains both calcium-rich oxide or silicate phases and fluorine-bearing microdomains that coexist.

References:

1. Xu, Y., Lv, Y., & Qian, C. (2023). Comprehensive multiphase visualization of steel slag and related research in cement: Detection technology and application. Construction and Building Materials, 386, 131572.

2. Adolfsson, D., Menad, N., Viggh, E., & Björkman, B. (2007). Steelmaking slags as raw material for sulphoaluminate belite cement. Advances in cement research, 19(4), 147-156.

3. Lee, H. H., Kwon, S. J., & Jang, S. U. (2010). Effects of PO2 at flux state on the fluorine dissolution from synthetic steelmaking slag in aqueous solution. ISIJ international, 50(1), 174-180.

4. Zhao, Q., Mei, X., Gao, L., Zhang, J., Wang, Z., Sun, L., ... & Saxén, H. (2021). Fundamental research on fluorine-free ladle furnace slag for axle steel of electric multiple unit vehicles. Metals, 11(12), 1973.

Isteri, V., Ohenoja, K., Rößler, C., Kletti, H., Tanskanen, P., Illikainen, M., ... & Fabritius, T. (2024). The effect of slag variability in the attempted manufacture of AYF (alite-ye'elimite-ferrite) cement clinker at both laboratory and pilot scale. CEMENT, 16, 100098.

1. Kishore, K., Sheikh, M. N., & Hadi, M. N. (2025). A critical analysis of electric arc furnace (EAF) slag for sustainable geopolymer concrete production. Materials Today Sustainability, 29, 101064.

2. Sagitov, A., Sherov, K., Mardonov, B., Akhmetov, Y., Ramazanova, Z., Ainabekova, S., ... & Esirkepov, A. (2023). Experimental Study of Improving the Durability of a Cup Cutter by Pre-Processing. Journal of Manufacturing and Materials Processing, 7(4), 146.